

A computer vision method to locate cold spots in foods in microwave sterilization processes

Ram Bhuwan Pandit, Juming Tang*, Frank Liu, Galina Mikhaylenko

Department of Biological Systems Engineering, Washington State University, 213 L J Smith Hall, Pullman, WA 99164-6120, USA

Received 17 March 2006; received in revised form 9 March 2007; accepted 19 March 2007

Abstract

A major challenge in developing advanced thermal processes based on electromagnetic heating is to determine the location of cold spots in foods. A rapid and reliable method was developed in this study with the aim to effectively locate the cold spot in model food sterilized in microwave systems. The developed method involved application of chemical marker M-2 yield to a model food, mashed potatoes, using computer vision system and an image processing software IMAQ Vision Builder to capture and analyze color patterns after thermal processes. A systematic study was conducted to establish relationships among M-2 yields, color values from captured images of cut food samples, and thermal lethality (F_0). Several factors including consistency of imaging background and positions of lights over the diffuser box were considered to standardize the method. To facilitate the comparative study of heating characteristic for different combinations of power levels and F_0 , a mapping scale using unheated and saturated mashed potato samples was developed by fixing the lowest and upper most gray-scale values. Color values equivalent to gray-level values were positively correlated to F_0 and M-2 yield. The specified cold spot location determined by computer vision method was validated in a 915 MHz single-mode microwave sterilization system. The results showed that the computer vision method can potentially be used as an effective tool in microwave sterilization process development for regulatory acceptance and industrial applications. © 2007 Pattern Recognition Society. Published by Elsevier Ltd. All rights reserved.

Keywords: Color values; Computer vision; Image processing; Chemical marker; Heating patterns; Microwave sterilization; Process validation; IMAQ vision builder; Cold spot

1. Introduction

Microwave sterilization holds promise to reduce process time and improve product quality [1,2]. Determination of cold spot locations in foods during microwave sterilization, however, is a major challenge for researchers in developing processes to ensure that the processed foods are safe to consumers. Computer simulation models can help in understanding the sterilization process [3,4]. Simulation models, however, require validation and may not always be reliable due to complexity of the coupling of heat transfer and dielectric heating in complex microwave sterilization cavities [5–7]. For any geometrically complex system used to produce safe foods for consumers, an

approach of double validation for process development was emphasized by US food regulatory organizations [8].

It is difficult to identify the cold spots in packaged foods during microwave sterilization processes by point temperature measurement methods. Chemical marker methods were studied as indirect means to evaluate relative heating absorptions in selected food systems [9–11]. Quantification of chemical markers M-1 and M-2 formed through Maillard reaction between amino acids and reducing sugar such as ribose and glucose required intensive laboratory analysis using high performance liquid chromatography (HPLC). For example, to analyze a 3-D heating pattern in processed mashed potato containing ribose in 10 oz trays with HPLC, two persons were needed for 2.5 days to quantify M-2 yield at 40 evenly distributed points in one tray. In process development, repeated tests are necessary with multiple trays. Analyzing M-2 yield in those many trays using HPLC became impractical. It was, therefore, desirable to develop a rapid and reliable method to capture the color

* Corresponding author. Tel.: +1 509 335 2140; fax: +1 509 335 2722.

E-mail address: jtang@wsu.edu (J. Tang)

URL: <http://www.microwaveheating.wsu.edu> (J. Tang).

Nomenclature			
$a(k, l)$	filters weight	M-2	chemical marker M-2
B	blue color value	m	size of matrix array
C	marker yield (mg/g of sample)	N	number of pixels
C_0	initial chemical marker yield (mg/g of sample)	R_0	universal gas constant at reference temperature (cal/mol K)
C_∞	chemical marker yield at saturation (mg/g of sample)	R	red color value
E_a	activation energy (kcal mol ⁻¹)	RGB	red, green, and blue color value
F_0	cumulative thermal lethality (min)	S	saturation
F	aperture value	$s_{in}(x, y)$	original gray-scale values
$f(x, y)$	light intensity of the points (x, y)	$s_{out}(x, y)$	output pixel values
$F(u, v)$	frequency domain of an image	t	time (min)
FFT	fast Fourier's transforms	T	temperature (°C)
g	gray level values	$T(t)$	temperature (K)
G	green color value	T_0	reference temperature
H	hue	u	horizontal spatial frequency
L	luminance	v	vertical spatial frequency
k_0	reaction constant at reference temperature	W	neighborhood around the pixel
		Π	multiplicative parameter

intensities of chemical markers (M-2) formation that reflect 3-D heating patterns.

A novel approach based on combination of chemical marker (M-2) yield and computer vision has been proposed as an option for evaluating the heating patterns of microwave-sterilized foods [12]. More research was needed to standardize the method and to establish correlation between color intensity and process lethality. In recent years, computer vision has reached wide-spread applications for quality inspection, classification, evaluation of products and processes in the agri-food industry [13–16]. An image processing based method has been studied as an optional technology for acquiring and analyzing an image to obtain information reflecting important product attributes [17–21]. A similar approach may be applied in thermal processing applications.

The specific objectives of this study were to: (1) establish a standard method that is not influenced by artifacts; (2) study the correlations among color values, chemical markers (M-2) yield and lethality (F_0); (3) use direct temperature measurement to validate this method in identifying the cold spot location in packaged foods processed in the microwave sterilization system.

The ultimate goal of this study was to develop an effective and reliable method for cold spot detection in support of FDA acceptance of microwave sterilization system and for future process development in industrial applications.

2. Materials and methods

2.1. Sample preparation

Mashed potato samples with 83.12% (wet basis) moisture content and 1.5% D-ribose were prepared similar as [6]. Eight grams of mashed potato sample was placed and sealed into custom-built aluminum containers (diameter 3.5 cm × height 1.4 cm)

with an air-tight lid for heating to elevated temperatures in oil baths. A type-T thermocouple was fitted into the lid of the container. The tip of the thermocouple was set to monitor sample temperature at the geometric center of the aluminum container during heating.

The cumulative lethality (F_0) is used to represent the degree of lethality of the target microorganism in a process equivalent to heating at 121 °C [12]. F_0 was calculated using the following formula [12]:

$$F_0 = \int_0^t 10^{(T-121.1)/z} dt \quad (1)$$

where T is the sample temperature in °C at any time t (min) during heating, z was taken as 10 °C for bacterial inactivation [22]. Value of z for chemical marker (M-2) formation in mashed potato was calculated as 32 °C using kinetics data [11].

2.2. Color palette and development of a new scale

A set of RGB (red, green, blue) values defines the rainbow palette of the IMAQ (Image Acquisition) program (National Instrument, Austin, TX, USA) in which varying degree of red, green, and blue colors are mathematically combined to produce a color value in gray-level range. National Instrument IMAQ Vision Builder 6.1 (National Instrument, Austin, TX, USA) assigned color value equivalent to gray-level value 255 to the darkest pixels of the image while color value to a lightest pixel was not fixed.

The developed scale was tested for several levels of cumulative lethality (F_0 , min) to obtain the distinctive color value for each level of F_0 . The gray-level value of the sample was transformed to a one-dimensional color value using the color scheme of Fig. 1. Since the full scale for color values varies depending upon the range of color intensity distribution in an image, for comparative study it was necessary to fix the gray-level

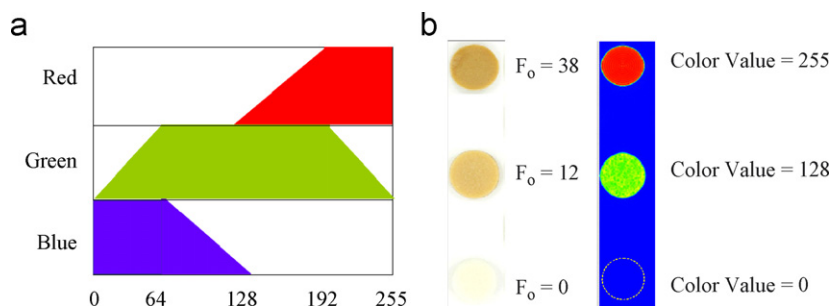


Fig. 1. Concept of converting the gray-level values to color values using rainbow color palette of IMAQ vision builder program and a method to fix the scale using mashed potato sample processed at different F_0 . (a) Rainbow palette. (b) New developed scale.

values to certain pixel intensity. This was done by selecting saturated and a unheated mashed potato as upper and lower limits to fix the full scale. Saturated samples were obtained when limiting factor amino acids in mashed potato were consumed during heating process and the formation of chemical marker would reach a saturation point. Beyond this point further heating would not result in significant chemical marker formation and color changes. The unheated mashed potato sample (marker M-2 yield = 0 mg/g sample) was used as the lowest point of the scale by setting color value to zero, and saturated mashed potato sample ($F_0 = 38$ min; marker yield = 0.268 mg/g sample) was used as the upper most point of the scale by setting color value to 255. A third point in the middle with color value 127 ± 5 ($F_0 = 12$ min) was set to improve the color resolution (Fig. 1).

Look-up table of the IMAQ Vision Builder software version 6.1 was used to maintain the brightness of the scale-sample to minimize the variation in the color value equivalent to gray scale value during color analysis.

2.3. Computer vision system

The computer vision system consisted of a light pod; helical compact fluorescent bulb; a digital camera with right-angle viewing attachment; automatic image acquisition software and computer vision software installed in a 1.6 GHz RAM Dell station (Fig. 2). A Nikon D 70 (Nikon Instrument, Melville, NY, USA) digital camera with 18–70 mm DX Nikkor lens was fitted on top of the Paterson Light Pod (Paterson Photographic Inc., Douglassville, GA, USA). The CCD (Charge Coupled Device) camera could move vertically on the stand to adjust the magnification and its distance from the sample. Nikon Capture 4 Editor version 4.3.0 (Nikon Instrument, Melville, NY, USA) software was used to acquire and download the images to a Dell Workstation.

2.4. Effect of lights positions on diffuser box

In the computer vision system, lights were mounted outside the light pod to maintain an even illumination inside the box. Four helical 26 W (120VAC, 60 Hz) bulbs (GE, Schenectady, NY, USA) were mounted on a stand at an angle of 45°

around a Paterson light pod “Cocoon” style medium diffusion shooting tent ($43 \times 50 \times 70$ cm). The diffusion light pod was used to prevent the incident monochromatic light source to the object. The incident light intensity inside the diffuser box was measured using a Sekonic exposure meter, FLASH-MATE L-308BII (Sekonic, Elmsford, NY, USA). High quality images were captured by matching the exposure meter readings, F (Aperture value = 30) and f/s (number of frame per second = 11), to Nikon D 70 digital camera through manual setting.

Computer vision analysis was performed to test the consistency in background for each image. To evaluate the effect of light positions on heating patterns, lights were mounted at top, middle and bottom positions of the light pod. Computer vision patterns for five samples heated to 110, 116, 121, 126 and 131°C temperatures were compared at each position of lights to investigate the affect of light position. Images of the heated samples taken at each position were analyzed using IMAQ Vision Builder software to determine the RGB value equivalent to a gray-scale value.

2.5. Color value, M-2 yield and F_0 relationship

2.5.1. Sample preparation and HPLC analysis

Since the activation energy of chemical marker formation in mashed potato $E_a = 22.23 \pm 1.54$ kcal/mol is different from that of bacterial inactivation ($E_a = 80 \pm 10$ kcal/mol) [11], it was anticipated that time-temperature history for mashed potato samples may affect the chemical marker yield even for the same final F_0 . Due to these variables two different pathways: (1) direct heating to a set temperature and (2) holding at 121°C for different F_0 were considered in this study. In the first set of tests, samples sealed in aluminum containers were heated to 110, 116, 121, 126, and 131°C temperatures (T) in an oil-bath to reach different levels of F_0 . In another set of tests, oil-bath temperature was set at 121°C and samples were held for a different period of time to cumulative lethality (F_0) of 1.5, 3, 6, 9, 12, 15 and 18 min. The samples were then rapidly cooled by immersing the aluminum containers into crushed ice. The purpose of fast cooling was to minimize additional cumulative lethality (F_0) after reaching the desired F_0 . Each experiment condition was repeated twice. Temperature and F_0 of the heated samples were monitored using data logging software

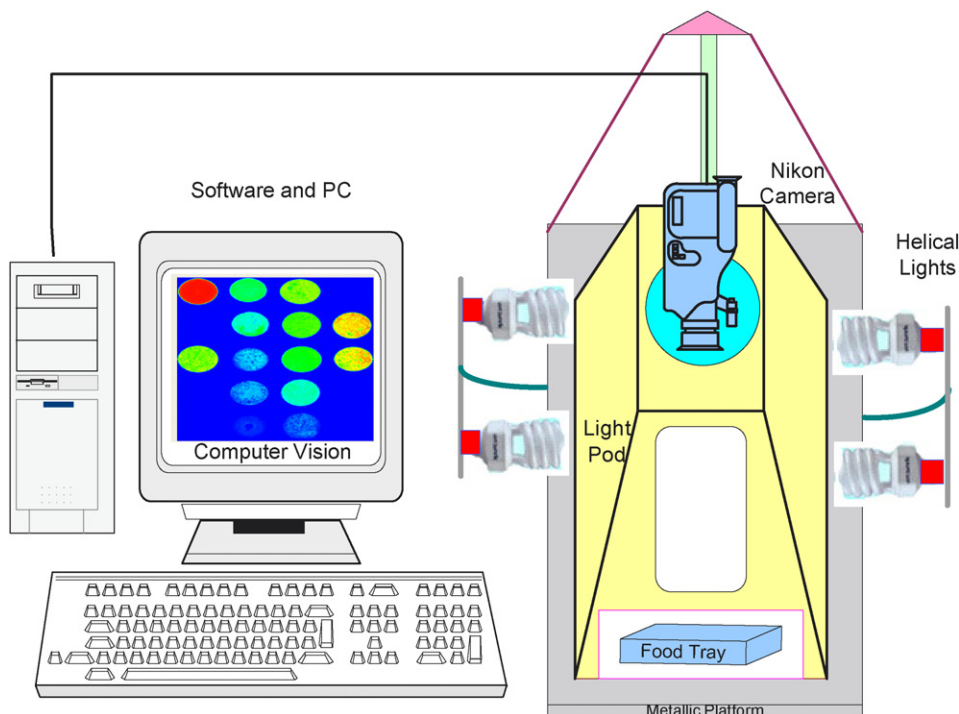


Fig. 2. Computer vision system designed in this study.

MS Visual Basic 6 with measurement-computing software Active X, Omega IDRX thermocouple (Omega Engineering Inc., Stamford, CT, USA) isolator controls, and hardware with serial output mounted on a personal computer. Software was logging data at an interval of 6 s.

Chemical marker M-2 yield for both sets of samples were determined using the Agilent 1100 HPLC system (Agilent Technology, Palo Alto, CA, USA). Before the analyses, samples weighing between 0.20 and 0.21 g were ground in 2 ml extraction buffer (10 mM sulphuric acid and 5 mM citric acid). Sample extraction and HPLC analysis procedures were the same as described [11]. Additionally, chemical marker (M-2) yield during heating process was predicted from measured temperature using the mathematical equation [9]:

$$C(t) = C_{\infty} - (C_{\infty} - C_0) \times \exp \left\{ \int_0^t -k_0 \exp \left(-\frac{E_a}{R_0} \left[\frac{1}{T(t)} - \frac{1}{T_0} \right] \right) dt \right\}, \quad (2)$$

where $C(t)$ is marker yield at any time, C_{∞} marker yield at saturation (0.268 mg/g sample), E_a is energy of activation (22.23 kcal mol⁻¹ K⁻¹), R_0 is molar gas constant (1.988 cal mol⁻¹ K⁻¹), $T(t)$ is recorded time-temperature history at the measured point (K), and T_0 is reference temperature (396.7 K). Initial marker yield before heating, C_0 , was considered to be zero for freshly made mashed potato samples containing 1.5% D-ribose. Experiments were also conducted to compare the M-2 yield of samples taken from the middle point of the container and samples taken by mixing the whole container (3.5 × 1.4 cm) for HPLC analysis.

2.5.2. Image acquisition and image editing using Adobe Photoshop

Nikon's Capture camera control tool was used for automatically acquiring and downloading the images. Sizes of the images taken were 3008 × 2000 with 24 bit per pixel, and were saved in Joint Photographic Experts Group (JPEG) format.

Adobe Photoshop CS version 8.0 (Adobe Systems, San Jose, CA, USA) was used to insert scale images and images to be analyzed into one package. A 20 × 25 cm automatic picture package was divided into 5 × 4 layouts [23]. The first column of the layouts was reserved for the scale samples and other columns were used for images to be analyzed for heating patterns. Resolution of images in picture package was set to 500 pixels per inch.

2.5.3. Functions in computer vision script

A computer vision script was developed through interactive programming to determine the color patterns of heated samples. Developed script in IMAQ Vision Builder contains functions as shown in Fig. 3. Selection of those function tools were made to meet the desired output, as a result of the sequential mathematical computation over original pixels of an image. Main functions are described in details in the following:

(i) *Look-up Table*—Look-up Tables (LuT) was used to set the brightness of the scale samples. An image (I) in rectangular matrix was defined as [24]:

$$I = f[s_{in}(x, y)], \quad (3)$$

where x is row index and y is column index. The original gray-scale values $s_{in}(x, y)$ can be assigned any value out of the

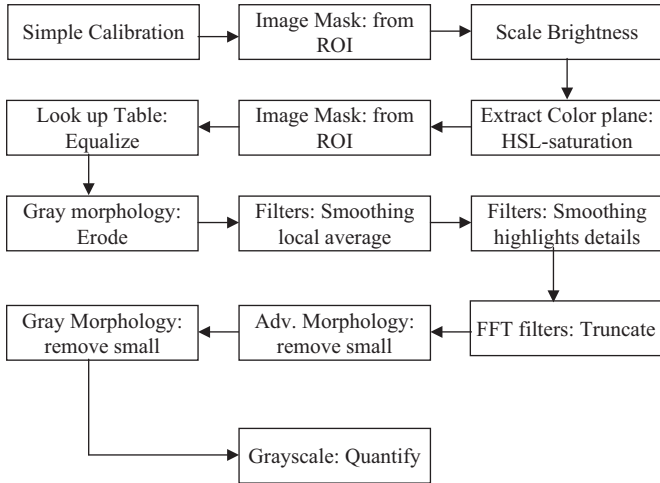


Fig. 3. Functions of the developed IMAQ Vision Builder script for heating pattern analysis.

gray-scale set $g = \{0, 1, \dots, 255\}$ for an 8-bit image. Resulting set of output values $s_{out}(x, y)$ using LuT would be

$$s_{out}(x, y) = f[s_{in}(x, y)]. \quad (4)$$

For each value of g , function $f(g)$ will have 256 possible values in a look-up table, therefore

$$\text{LuT}(g) = f(g). \quad (5)$$

In that case, the computed output of the LuT function becomes:

$$s_{out}(x, y) = \text{LuT}(s_{in}(x, y)). \quad (6)$$

(ii) *Extract color planes: HSL*—IMAQ Vision Builder provides a pre-defined unique feature based on this concept to represent the gray-level value of a pixel into corresponding one dimensional color value comprised of varying amounts of red, green, and blue (Fig. 1). Color plane HSL (hue, saturation, and luminance) saturation was extracted from each image to adjust the lowest gray-level value to the lightest pixel and the highest gray-level value to the darkest pixel of an image. The coordinate system for HSL color space is cylindrical. The hue (H) value runs from 0° to 360° , the saturation (S) ranges from 0 to 1, and luminance (L) also ranges from 0 to 1, where 0 is black and 1 is white. Following equations describe the nonlinear transformation that maps the RGB color space to the HSL color space [25]:

$$L = 0.3 \times R + 0.59 \times G + 0.11 \times B, \quad (7)$$

$$V2 = \sqrt{3} \times (G - B), \quad (8)$$

$$V1 = 2 \times R - G - B, \quad (9)$$

$$H = 256 \times \tan^{-1} \left(\frac{V2}{V1} \right) / (2 \times \Pi), \quad (10)$$

$$S = 255 \times \left(1 - \frac{3 \times \min(R, G, B)}{(R + G + B)} \right), \quad (11)$$

where Π is multiplicative parameters.

(iii) *Gray morphology: erosion and dilation*—These two functions are fundamentals for almost all morphological operations. Dilation increases the brightness of pixels surrounded by proximate pixels with a higher intensity, while erosion is a function that basically reduces brightness of each pixel that is surrounded by proximate pixels with a lower intensity. In erosion, the value of output pixels is set to the minimum of coefficients $s_{in}(x, y)$ as [26,24]

$$s_{out}(x, y) = \min(s_{in}(x, y)) \quad (12)$$

while in dilations, output of the pixels is set to the maximum value of coefficients $s_{in}(x, y)$ as

$$s_{out}(x, y) = \max(s_{in}(x, y)). \quad (13)$$

(iv) *Filters: smoothing local average*—Averaging of the brightness intensity of a pixel was performed by taking the weighted average of the proximate pixels. The output image in that case would be expressed as [27,28]

$$g(m, n) = \sum \sum a(k, 1) f(m-k, n-1), \quad (k, 1) \in W, \quad (14)$$

where $f(m, n)$ and $g(m, n)$ are the input and output images, respectively, W is the neighborhood of the pixel at location (m, n) , and $a(k, 1)$ are the filter weights assigned. All weights were assigned equal values in this study; and therefore Eq. (14) was reduced to

$$g(m, n) = \frac{1}{N} \sum \sum f(m-k, n-1), \quad (k, 1) \in W, \quad (15)$$

where N is the number of pixels in the proximate of W . The purpose of spatial averaging operation on an image was to smooth the noise. In case of an observed image, it was defined as

$$g(m, n) = f(m, n) + \eta(m, n) \quad (16)$$

the spatial average of the image was calculated as

$$g(m, n) = \frac{1}{N} \sum \sum f(m-k, n-1) + \bar{\eta}(m, n), \quad (k, 1) \in W, \quad (17)$$

where $\bar{\eta}(m, n)$ was an average of the noise component $\eta(m, n)$ in the spatial domain of the image.

(v) *Filters: smoothing highlight details*—Filtering improved the quality of the image by calculating the new pixel value by using the original pixel value and those of its proximities. Mathematical computation on each pixel was performed by using the equation [24,29]

$$s_{out}(x, y) = \frac{1}{m^2} \sum_{u=0}^{m-1} \sum_{v=0}^{m-1} s_{in}(x+k-u, y+k-v) \times f(u, v). \quad (18)$$

The output pixel values $s_{out}(x, y)$ depends on the size of kernel matrix $(m \times m)$. IMAQ has three predefined kernel matrices of size $m = 3, 5$ and 7 . Under this study, most of the calculations were done with $m = 3$ and parameter k was defined as

$$k = \frac{(m-1)}{2}. \quad (19)$$

Indices u , and v depend on x and y with k in terms of filter kernel function [29]. In case of kernel size 3×3 , all nine neighboring pixels were represented as

$$\mathbf{F} = (f(u, v)) = \begin{pmatrix} f(0, 0) & f(0, 1) & f(0, 2) \\ f(1, 0) & f(1, 1) & f(1, 2) \\ f(2, 0) & f(2, 1) & f(2, 2) \end{pmatrix}. \quad (20)$$

Using indices x and y Eq. (20) can be elaborated as

$$\mathbf{F} = \begin{pmatrix} f(x-1, y-1) & f(x, y-1) & f(x+1, y-1) \\ f(x-1, y) & f(x, y) & f(x+1, y) \\ f(x-1, y+1) & f(x, y+1) & f(x+1, y+1) \end{pmatrix} \quad (21)$$

this includes a pixel (x, y) with its eight proximities pixels.

(vi) *Fast Fourier transforms (FFT: Low pass truncation)*: The 2D *Fourier transforms* transforms a spatial function $f(x, y)$ of an image into frequency domain $F(u, v)$, which in continuous domain, was defined as [25,24,30]:

$$F(u, v) = \int_{-\infty}^{\infty} \int_{-\infty}^{\infty} f(x, y) e^{-j2\pi(xu+vy)} dx dy. \quad (22)$$

The exponential function was expressed using Euler's identity as

$$\exp(-j2\pi(xu + yv)) = \cos(2\pi(xu + yv)) - j \sin(2\pi(xu + yv)), \quad (23)$$

where $f(x, y)$ was the light intensity of the points (x, y) , and u, v were the horizontal and vertical spatial frequencies. Eq. (22) implies that the function $f(x, y)$ is essentially multiplied by the terms $\cos(2\pi ux) \cos(2\pi vy)$, $\sin(2\pi ux) \sin(2\pi vy)$, $\sin(2\pi ux) \cos(2\pi vy)$, and $\cos(2\pi ux) \sin(2\pi vy)$. In case of a symmetric function, along both the X - and Y -axes, Fourier transform of $f(x, y)$ involves the multiplication of $\cos(2\pi ux) \cos(2\pi vy)$ term only. But in this study, the $f(x, y)$ multiplication involved all four terms due to asymmetric images. Inversely *fast Fourier transformed* $F(u, v)$ can be transformed back into a spatial image $f(x, y)$ of resolution $N \times M$:

$$f(x, y) = \sum_{u=0}^{N-1} \sum_{v=0}^{M-1} F(u, v) e^{j2\pi(ux/N-vy/M)}, \quad (24)$$

where $F(u, v)$ consists of an infinite sum of sine and cosine terms, which are determined by the corresponding frequency. For the given set of u and v all values of $f(x, y)$ contribute to $F(u, v)$. The FFT computation on the image before quantifying the RGB values took between 2 and 10 minutes depending upon the size of the image to be analyzed for cold spot detection.

2.6. Computer vision heating patterns for food samples using IMAQ Vision Builder

A picture package including images of mashed potato samples in Adobe Photoshop was analyzed using IMAQ Vision Builder program. Brightness of the scale samples were fixed using look-up table, and regions of interest (ROI) were selected

using image mask. A developed function script (Fig. 3) was run to determine the heating patterns. Forty (8×5) rectangular grids were generated on the heating pattern of each tray. The color values of the grids for each tray were directly extracted to Microsoft Office program Excel (MS Office-2003, USA). Similar steps were followed to collect color values from other images of the package. Using MS Excel, a grid with lowest color value was selected among all of the grids and detected as the cold spot region of the microwave sterilization process.

3. Results and discussion

3.1. Computer vision color patterns

Colors of heated samples were analyzed by referencing the developed scale in each picture package using Adobe Photoshop. Computer vision showed different color as a result of different M-2 yield at each level of F_0 (Fig. 4). HPLC analysis revealed that the sample held at 121°C for $F_0 = 6$ min had much higher chemical marker yield (0.089 mg/g) than a sample directly heated to 126°C (0.029 mg/g) for a similar level of F_0 (Table 1). Due to a short heating duration and higher temperature than 121°C , direct heating to 126, 131°C temperatures leads to higher F_0 in the tested samples, while chemical marker yields were all comparatively lower. This is because of the earlier stated difference between the activation energy for M-2 formation and that for thermal inactivation of *C. botulinum* spores used in F_0 calculation.

It is clear that correlation between M-2 formation and F_0 are dependent of temperature pathway which will be discussed in details.

Our test results also showed that positions of lights around the diffuser box had no effect on the color images captured by the computer vision system (Fig. 5). Statistical analysis (SAS, Institutes Inc., Cary, NC, USA) at 95% level of significance showed no significant difference in measured color value of the images taken at three different light positions. A separate study was also conducted to compare the color values of the sample analyzed right after heating and samples stored maintaining a protocol (storage protocol: 1 h at -35°C , 12 h at 5°C , and 1 h again -35°C). This study showed no significant difference (P -value > 0.98) in color value for both set of samples.

3.2. Color value equivalent to gray-level value and M-2 yield

Gray-scale quantification tool was used to obtain the color value equivalent to a gray-level value for each sample. A representative color value along with the standard deviation of selected ROI (Region of Interest) was obtained using IMAQ Vision Builder. Our tests showed that chemical marker yield of the sub-sample taken at center of the sample and that of the mixed whole sample in the same container was not significantly different (P -value = 0.985) (SAS, Institutes Inc., Cary, NC, USA). To expedite the extraction procedure, a sub-sample from the middle section of the treated sample was taken at each level of F_0 for determination of the M-2 yield using HPLC. M-2 yields of analyzed samples were positively correlated with

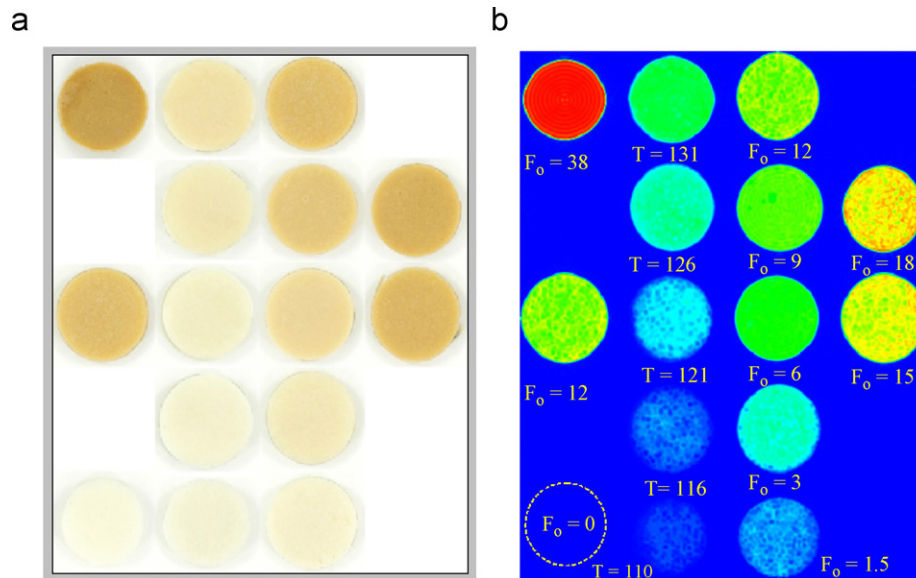


Fig. 4. Computer vision patterns for mashed potato samples heated to a set temperature (T) or held to 121 °C for different F_0 . (a) Original sample. (b) Computer vision patterns.

Table 1

Color values equivalent to gray-scale values and chemical marker M-2 yield for two different heating conditions, each point represents mean of two replicates

Data collected for	Temperature or target F_0	F_0 (min)	M-2 yield (mg/g of sample)	Color value equivalent to Gray-level
Ramp up to temperature levels (°C)	110.00	0.15 ± 0.00	0.005 ± 0.004	10.17 ± 2.48
	116.00	0.53 ± 0.15	0.013 ± 0.005	29.70 ± 8.65
	121.00	1.85 ± 0.03	0.021 ± 0.008	47.78 ± 7.71
	126.00	6.17 ± 0.28	0.029 ± 0.001	84.69 ± 2.16
	131.00	17.81 ± 3.83	0.053 ± 0.011	108.78 ± 3.13
Holding at 121 °C for F_0 (min)	1.50	1.57 ± 0.09	0.016 ± 0.001	29.08 ± 9.55
	3.00	2.98 ± 0.10	0.034 ± 0.004	78.70 ± 3.26
	6.00	6.08 ± 0.01	0.089 ± 0.001	125.84 ± 2.28
	9.00	9.05 ± 0.08	0.124 ± 0.008	143.54 ± 5.25
	12.00	12.02 ± 0.04	0.152 ± 0.003	158.01 ± 0.04
	15.00	15.05 ± 0.04	0.167 ± 0.002	184.68 ± 3.57
	18.00	17.98 ± 0.04	0.201 ± 0.014	196.05 ± 2.28

the cumulative thermal lethality F_0 (Fig. 6). M-2 yields of the samples were also correlated with imagine parameter, color value, to establish a relationship (Table 1). Results showed a unique positive correlation between M-2 yield and color values (Fig. 7) regardless of heating pathways. This indicates that computer visions based on the color value equivalent to gray scale can uniquely reflect M-2 yields in thermal processes.

3.3. Color value equivalent to gray-level value and F_0

The color values measured for each sample using IMAQ Vision Builder were plotted against F_0 values. Two different positively correlated trends, one for samples heated by holding at 121 °C and another for samples directly heated to a set temperature (ramp up), were obtained (Fig. 8). For each different heating pathway, plotted result showed that each level of F_0

will lead to a unique M-2 yield and color value (Figs. 6–8). These relationships between M-2 yield vs. F_0 , and color value vs. F_0 are unique for a given condition of heating. Based on these relationships, by referring to a scale, color value can be used as a representative for the thermal lethality (F_0) and chemical marker (M-2) yield.

4. Validation of locations specified by computer vision

In order to validate the accuracy of the cold and the hot spot locations determined by the computer vision method, experiments were conducted in a 915 MHz single-mode pilot-scale microwave sterilization system in two replicates. Thermo wells that separated sealed sample from fiber-optic sensors were fitted into the tray at the measured distance of cold and hot spot locations. Each tray was filled with 200 g of mashed potato

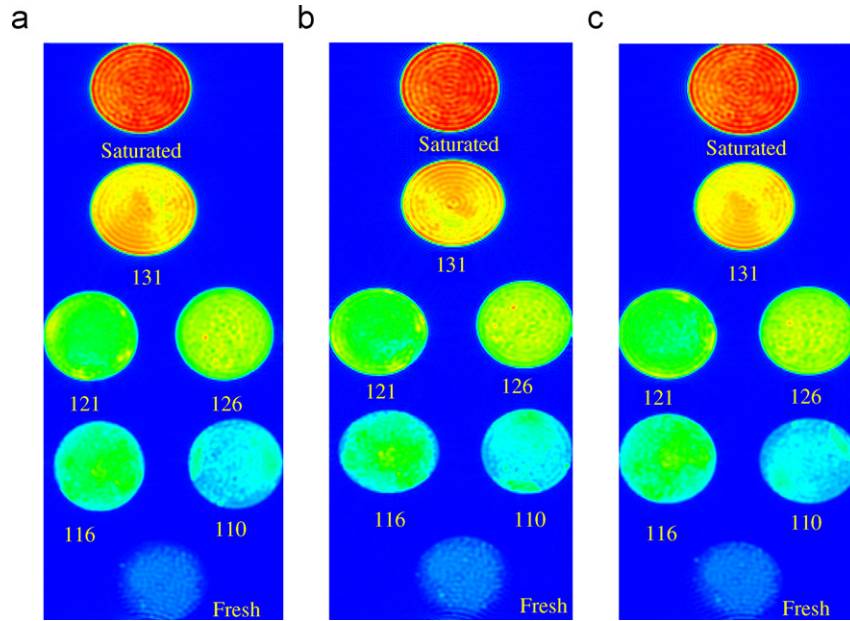


Fig. 5. Comparison of computer vision color patterns with mashed potato samples heated to different temperature levels for three positions (bottom, middle and top) of lights. Number denotes the set temperature to which sample was heated. (a) Bottom. (b) Middle. (c) Top.

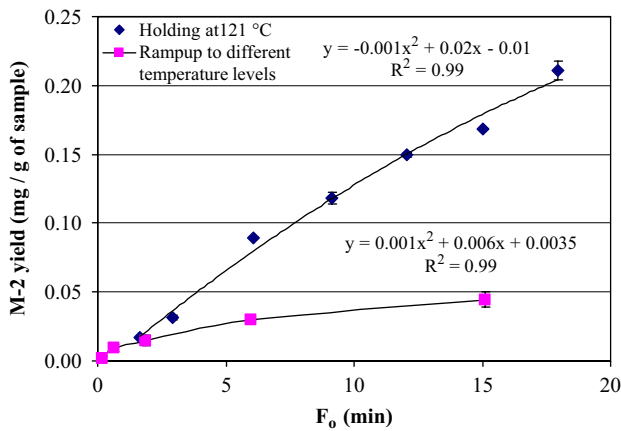


Fig. 6. M-2 yield and F_0 correlation with mashed potato samples heated to different set temperature (ramp up) levels or held at 121 °C for different F_0 , data points represent means for two replicates.

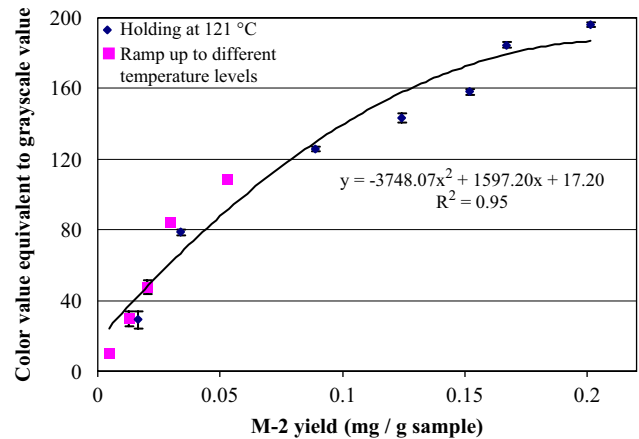


Fig. 7. Color value and M-2 yield relationship with mashed potato samples heated to different set temperatures (ramp up) levels or held at 121 °C for different F_0 , data points represent means for two replicates.

sample mixed with 1.5% D-ribose and then vacuum-sealed at 18 in of Hg vacuum. Trays were set on an Ultem support and a proper speed was chosen to move the tray support from the loading section to the holding section through two single-mode microwave cavities. Water at 125 °C was circulated across the tray support inside the pressurized microwave cavities at a flow rate of 35 lpm. Fiber optic temperature sensors inserted into the thermo wells measured temperature at the specified cold and hot spot locations identified by computer vision method. The experiments were conducted at a 2.67 kW microwave power level. The measured temperature confirmed that the temperature measured at the perceived hot spot was indeed always higher than the cold spot for all tests, as shown by a representative curve in Fig. 9.

To further confirm the locations of the cold spots relative to other parts of the tray, additional 13 tests were conducted. In each of the tests, four pre-calibrated optic sensors were placed in a sample tray during the microwave sterilization process. One of the sensors was always inserted at the cold spot identified by the computer vision method while the others were placed in three different locations. Compiling all the measured temperatures from the 13 tests, provided temperature profile for a total of 40 different points (8×5) evenly distributed in the middle layer of a tray. Computer vision patterns and temperature mapping, of middle layers, obtained using fiber optics are compared in Fig. 10. It shows that heating pattern and cold spot location obtained by both the methods were concordant. This indicates that the novel computer vision method indeed reliably reveal

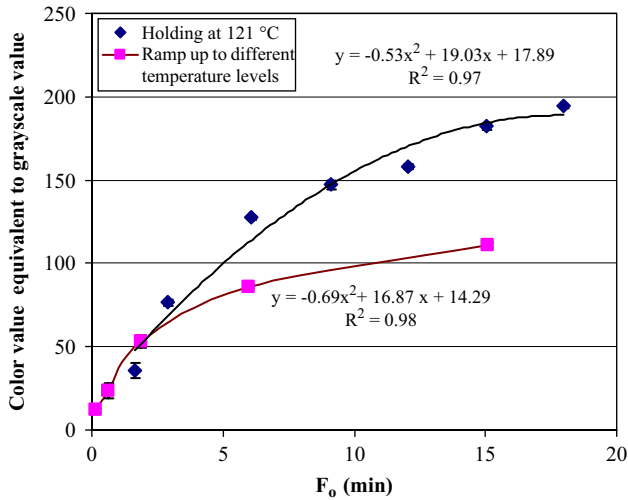


Fig. 8. Color value and F_0 relationship with mashed potato samples heated to different set temperatures (ramp up) levels or held at 121 °C for different F_0 , data points represent means for two replicates.

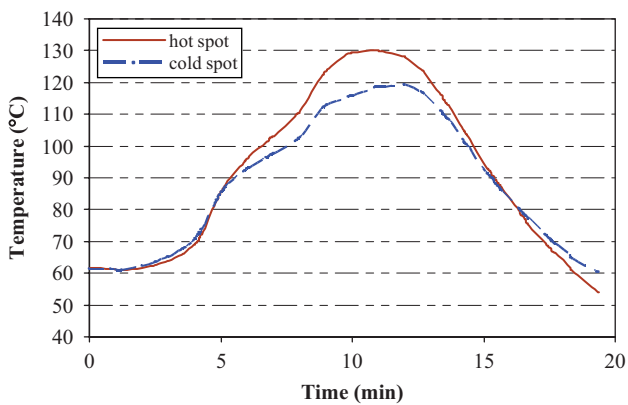


Fig. 9. Validation of cold and hot spots locations specified by computer vision method in 10 oz trays during microwave sterilization at 2.67 kW power level, typical temperature profile from repeated tests in the middle layer of the tray.

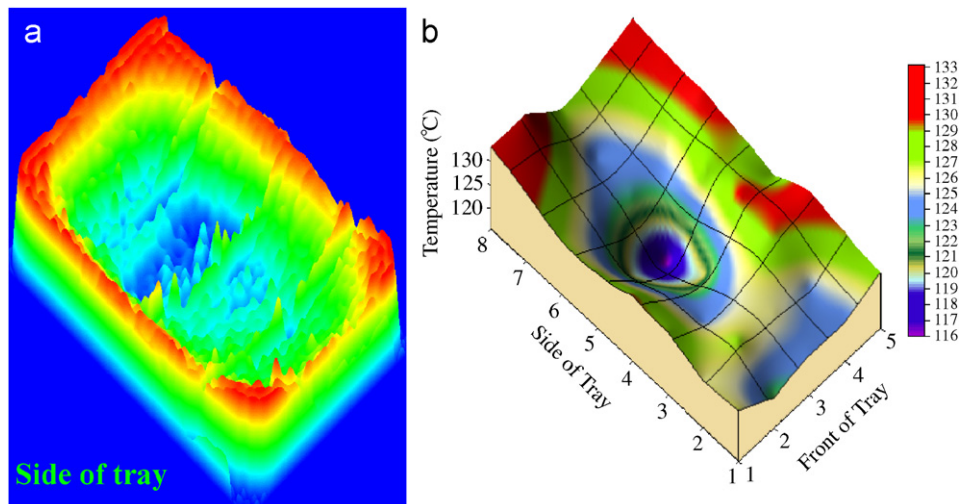


Fig. 10. Matching of the experimental and developed method heating patterns for the middle layer of a 10 oz tray with mashed potato processed at 2.67 kW microwave power level. (a) Heating pattern by developed computer vision method. (b) Temperature distribution measured by fiber optic probes.

the cold spots in foods and can be used to study general heating patterns in foods after microwave sterilization processes.

5. Conclusions

The designed computer vision system provided consistent background for the images. The developed scale can be used to compare the heating patterns of microwave-sterilized foods for combinations of power levels and F_0 . Shooting tent worked well as an effective diffuser, and positions of lights for a fixed setting of exposure intensity had no influence on the heating patterns.

Color value equivalent to gray scale value was positively correlated with chemical marker yield and cumulative thermal lethality (F_0). For a given F_0 , chemical marker (M-2) yield of the samples heated directly to 126, 131 °C temperatures were lower than holding the sample at 121 °C. Separate pathway provides different correlation between M-2 yield and F_0 . But correlation between color values and M-2 yield are independent of heating pathway. Based on these relationships, a computer vision method was developed to identify the cold and the hot spot regions of a processed food sample. Validation tests confirmed that the computer vision method based on chemical marker M-2 yield can accurately determine the location of cold spots. The developed knowledge base will support application of this method for evaluation of microwave sterilization processes.

Currently this method is being used to locate the cold spots in salmon with sauce to develop filing documents for FDA acceptance of the 915 MHz microwave sterilization processes.

Acknowledgments

This research work was supported by the US Army Natick Soldier Center, Natick, MA and the Washington State University Agricultural Research Center, Pullman WA.

References

- [1] D. Guan, V.C.F. Plotka, S. Clark, J. Tang, Sensory evaluation of microwave treated macaroni and cheese, *J. Food Process. Preserv.* 26 (5) (2002) 307–322.
- [2] D. Guan, P. Gray, D.H. Kang, J. Tang, B. Shafer, K. Ito, F. Younce, T.C.S. Yang, Microbiological validation of microwave-circulated water combination heating technology by inoculated pack studies, *J. Food Sci.* 68 (4) (2003) 1428–1432.
- [3] S.K. Pathak, F. Liu, J. Tang, Finite difference domain (FDTD) characterization of a single mode applicator, *J. Microwave Power Electromagn. Energy* 30 (1) (2003) 1–12.
- [4] H. Zhang, A.K. Datta, Coupled electromagnetism and thermal modeling of microwave oven heating of foods, *Int. Microwave Power Inst.* 35 (2) (2000) 71–85.
- [5] K.G. Ayappa, H.T. Davis, E.A. Davis, J. Gordon, Two-dimensional finite element analysis of microwave heating, *AIChE J.* 38 (10) (1991) 1577–1592.
- [6] R.B. Pandit, S. Prasad, Finite element analysis of microwave heating of potato-transient temperature profiles, *J. Food Eng.* 60 (2003) 193–202.
- [7] V.R. Romano, F. Marra, U. Tammaro, Modeling of microwave heating of foodstuff: study on the influence of sample dimensions with FEM approach, *J. Food Eng.* 71 (2005) 233–241.
- [8] Food and Drug Administrations, 2005, Thermally processed low-acid foods packaged in hermetically sealed containers (Chapter 1). Available from: (<http://www.fda.gov/>) (Accessed March, 2005).
- [9] M.H. Lau, J. Tang, I.A. Taub, T.C.S. Yang, C.G. Edwards, R. Mao, Kinetics of chemical marker formation in whey protein gels for studying microwave sterilization, *J. Food Eng.* 60 (4) (2003) 397–405.
- [10] Y. Wang, M.H. Lau, J. Tang, R. Mao, Kinetics of chemical marker M-1 formation in whey protein gels for developing sterilization processes based on dielectric heating, *J. Food Eng.* 64 (2004) 111–118.
- [11] R.B. Pandit, J. Tang, G. Mikhaylenko, F. Liu, Kinetics of chemical marker M-2 formation in mashed potato—a tool to locate cold spots under microwave sterilization, *J. Food Eng.* 76 (3) (2006) 353–361.
- [12] R.B. Pandit, J. Tang, F. Liu, M. Pitts, Development of a novel approach to determine heating pattern using computer vision and chemical marker (M-2) yield, *J. Food Eng.* 78 (2) (2007) 522–528.
- [13] M.Z. Abdullah, L.C. Guan, K.C. Lim, A.A. Karim, The application of computer vision system and tomographic radar imaging for assessing physical properties of food, *J. Food Eng.* 61 (1) (2004) 125–135.
- [14] H.H. Wang, D.W. Sun, Melting characteristics of cheese: analysis of effects of cooking conditions using computer vision techniques, *J. Food Sci.* 51 (2002) 305–310.
- [15] K.L. Yam, S.E. Papadakis, A simple digital imaging method for measuring and analyzing color of food surfaces, *J. Food Eng.* 61 (2004) 137–142.
- [16] H. Hwang, B. Park, M. Nguyen, Y.R. Chen, Hybrid image processing for robust extraction of lean tissue on beef cut surfaces, *Comput. Electron. Agric.* 31 (1997) 17–29.
- [17] T. Brosnan, D.W. Sun, Improving quality inspection of food products by computer vision—a review, *J. Food Eng.* 61 (2004) 3–16.
- [18] S. Gunasekaran, Computer vision technology for food quality assurance, *Trends in Food Sci. Technol.* 7 (1996) 245–256.
- [19] D.J. Cheng, D.W. Sun, Pizza sauce spread classification using colour vision and support vector machines, *J. Food Eng.* 66 (2) (2005) 137–145.
- [20] J. Lu, J. Tan, P. Shatadal, D.E. Gerrard, Evaluation of pork color by using computer vision, *Meat Sci.* 56 (2000) 57–60.
- [21] B. Zion, A. Shklyar, I. Karplus, Sorting fish by computer vision, *Comput. Electron. Agric.* 23 (3) (1999) 175–187.
- [22] S.D. Holdsworth, Sterilization, pasteurization and cooking criteria, Thermal processing of packaged foods, Boundary Row, London: Blackie Academic and Professional, London, 1997, pp. 99–110.
- [23] Adobe System, Adobe Photoshop 7.0 User Guide, San Jose, CA, Adobe System, INC, 2002.
- [24] K. Thomas, Image processing with LabView and IMAQ vision, Image Processing, Prentice-Hall, Upper Saddle River, NJ, 2003.
- [25] IMAQ vision builder tutorials, National Instrument Corporation. Available from (<http://www.ni.com/>) (Accessed on January, 2004).
- [26] E.R. Davies, Machine Vision: Theory Algorithms and Practicalities, Academic Press, New York, 1997.
- [27] T. Acharya, A.K. Ray, Image Processing: Principles and Application, Wiley-Interscience Publication, Hoboken, NJ, 2005.
- [28] G.X. Ritter, J.N. Wilson, Handbook of Computer Vision Algorithms in Image Algebra, CRC Press, Boca Raton, NY, 2000.
- [29] X.T. Gerhard, N.W. Joseph, Handbook of Computer Vision Algorithms in Image Algebra, CRC Press, Boca Raton, NY, 1996.
- [30] L.G. Shapiro, G.C. Stockman, Computer Vision, Prentice-Hall, Upper Saddle River, New Jersey, 2001.

About the Author—RAM BHUWAN PANDIT received his Ph.D. in Food Engineering from Biological Systems Engineering Department of Washington State University in 2006. He received his M. Tech in Dairy and Food Engineering from Indian Institute of Technology, Kharagpur in 2002 and B.Tech in Agricultural Engineering from College of Agricultural Engineering, RAU, Pusa (India) in 2000. His research interests include application of computer vision, digital image processing and mathematical modeling of food processes and unit operations. Currently, he is working as post doctoral researcher in Food, Agricultural and Biological Engineering Department of The Ohio State University, Columbus, OH.

About the Author—JUMING TANG, Ph.D., is a Professor of Food Engineering in the Department of Biological Systems Engineering at Washington State University, Pullman, Washington. He teaches and conducts research in food processing engineering, thermal processing, and novel food preservation technologies. Dr. Tang has published over 130 peer reviewed scientific papers, over 10 book chapters and two books in the above areas. Dr. Tang is a Washington State University IMPACT Center Fellow and directs multi-disciplinary research programs related to development of novel food processing technologies based on microwave and radio frequency energies and non-chemical pest post harvest control of agricultural commodities in international trades. He is a member of the Board of Governors for the International Institute of Microwave Power and a professional member of the Institute of Food Technologists, American Society of Agricultural and Biological Engineers and Institute for Thermal Processing Specialists.

About the Author—FRANK LIU, Ph.D., is a Research Associate in the Department of Biological Systems Engineering at Washington State University, Pullman, Washington. He received Ph.D. degree in Chemical Engineering from Dalian University of Science and Technology, Dalian China in 1987 and B.S. degree in Chemical Engineering from Qingdao University of Science and Technology, Qingdao, China in 1978. He has more than 10 years research experience in designing and developing of industrial scale microwave sterilization or pasteurization units for food industries. His research interests include digital image processing, pattern recognition, fuzzy logic for automatic control and computer modeling.

About the Author—GALINA MIKHAYLENKO is an Associate in Research in the Department of Biological Systems Engineering at Washington State University. Her area of expertise includes food technology and image processing.